

# A novel model of the pulse decay method for measurement of local tissue blood perfusion

Kun Yang\*, Wei Liu

*Department of Power Engineering, Huazhong University of Science and Technology, Wuhan, Hubei, 430074, China*

Received 23 May 2003; received in revised form 10 October 2003; accepted 20 October 2003

## Abstract

The blood perfusion of biological tissue is a basic parameter of physiology and medical engineering. A novel average temperature model (ATM) is presented in this paper to measure the blood perfusion of tissue based on the thermal pulse-decay method. Differing from the existing point source model (PSM) and spherical source model (SSM), the probe bead average temperature analytical solution is derived and used to estimate the blood perfusion. The blood perfusion prediction errors caused by the approximate assumptions used in each model are studied using the numerical experiment method. Contributions of the tissue parameters, probe thermistor bead parameters, and measurement parameters, such as tissue thermal conductivity, tissue thermal diffusivity, blood perfusion rate, bead thermal conductivity, bead radius, measurement time, and thermal pulse length are discussed. The predicting accuracy of the ATM model is compared with the PSM model and SSM model. The results show that, for all the cases tested, the ATM model is better than the other two.

© 2003 IPPEM. Published by Elsevier Ltd. All rights reserved.

*Keywords:* Blood perfusion; Thermal pulse decay method; Average temperature model; Prediction error; Numerical experiment

## 1. Introduction

The blood perfusion of biological tissue is a basic parameter of physiology and medical engineering, which plays an important role for the mass and energy transfer in biological tissue (such as the local transport of nutrients, oxygen, drug, and heat), also has a considerable influence on the temperature distribution in biological tissue. The estimation of tissue blood perfusion is considered as a key task for the establishment and validation of bio-heat transfer equation [1,2], for understanding of the thermal response of the biological tissue under outer-supplied heating energy [3,4], for knowledge of the physiological functions of normal and pathological tissue [5,6], as well as for disease diagnostics and therapies. Particularly during the thermal therapy of cancer, the temperature field should be

accurately estimated and controlled in order to achieve an effective treatment. Thereby, the blood perfusion of both the normal and the tumor tissue should be measured, before and during the hyperthermia treatment, and then the heat source could be organized more reasonably [7–9].

Due to the effects of blood perfusion on the mass and heat transfer characteristics of the biological tissue, various techniques have been used for blood perfusion measurement according to the thermal response of the biological tissue [10–17], among which the pulse-decay method does not require any stop-flow or post mortem measurements [13], neither require an additional control module to achieve some prescribed measurement conditions, thus is simpler to be applied. According to the pulse-decay method [13], a probe with a thermistor bead mounted at the tip is inserted into the tissue of interest, which serves first as a power source and then as a temperature sensor. The method is based on comparing the measured and model simulated temperature decay following a power pulse insertion through the thermistor bead to estimate the blood perfusion.

\* Corresponding author. Tel.: +86-27-87542618; fax: +86-27-87540724.

E-mail address: kuny8@sina.com.cn (K. Yang).

By presuming the measured tissue is small enough to allow uniform blood perfusion rate and thermal properties within it, but sufficiently large to simulate the bead as a heating point source, Arkin et al. [13] introduced a point source model (PSM) and derived an analytical solution of the temperature decay. Based on the least-squares regression, the difference between the measured temperature and the theoretically calculated temperature can be minimized to determine the blood perfusion. A sensitivity analysis of the thermal pulse decay method (using the point source model) has been performed by Arkin et al. [18], the errors in the calculated blood perfusion caused by the error in measured temperature, the error in measured supplied power, the error in measured pulse length, as well as the finite size of the heating probe were discussed, and an “optimal” measurement time interval was found. Considering the effects of the finite size of the probe bead, Diederich et al. [19] introduced a spherical source model (SSM) for the thermal pulse decay method, which assumed the heating source was spherically symmetric with a finite radius, the analytical solution for the central temperature of the probe bead was derived and was used to estimate the blood perfusion. Also, the model errors of both the PSM model and SSM model were compared by using the transient temperature decay data generated from a reference model, and the results disclosed the accuracy of the SSM model were better than the PSM model in all cases tested. However, in point of fact, the thermistor bead sensing temperature is the average temperature of the whole probe bead [10], and SSM model replaces the probe average temperature with the probe central temperature when the analytical solution of probe bead central temperature is used to estimate the blood perfusion. In this paper, a novel model named average temperature model (ATM) for the thermal pulse-decay method is presented, the solution of the probe bead average temperature is obtained based on the Pennes’ bio-heat Eq. [20] and used to estimate the blood perfusion, thus the prediction accuracy is improved. Furthermore, the accuracy of the PSM model, the SSM model, and the ATM model are discussed by using the numerical experiment method.

## 2. Descriptions of the PSM model, the SSM model, and the ATM model

The well-known Pennes’ equation is used to model the heat transfer in the biological tissue [20].

$$\rho_t C_t \frac{\partial T_t}{\partial t} = k_t \frac{1}{r^2} \frac{\partial}{\partial r} \left( r^2 \frac{\partial T_t}{\partial r} \right) + W_b C_b (T_a - T_t) + q_m + q_b \quad (1)$$

where  $T_t = T_t(r, t)$  is the temperature of tissue;  $T_a$  is the

supplying arterial blood temperature;  $\rho_t$ ,  $C_t$ ,  $k_t$ , denote density, specific heat, and thermal conductivity of tissue;  $C_b$  is the specific heat of blood;  $q_m$  is the steady state metabolic heat rate;  $q_b$  is the rate of heat inserted into the tissue;  $W_b$  is the blood perfusion rate.

The respective steady state bio-heat equation is

$$k_t \frac{1}{r^2} \frac{\partial}{\partial r} \left( r^2 \frac{\partial T_t(r, 0)}{\partial r} \right) + W_b C_b (T_a - T_t(r, 0)) + q_m = 0. \quad (2)$$

Subtracting Eq. (2) from Eq. (1), we have

$$\rho_t C_t \frac{\partial \theta}{\partial t} = k_t \frac{1}{r^2} \frac{\partial}{\partial r} \left( r^2 \frac{\partial \theta}{\partial r} \right) - W_b C_b \theta + q_b \quad (3)$$

where  $\theta(r, t) = T_t(r, t) - T_t(r, 0)$  and the relevant initial and boundary conditions are  $\theta(r, 0) = 0$ ;  $\theta(\infty, t) = 0$ .

Arkin [13] assumed the probe bead is a heating point source that inserts heat into the tissue for a given interval, and  $q_b$  takes the form:

$$q_b = q_p \cdot \delta(r) \cdot [1 - H(t - t_p)] \quad (4)$$

where  $t_p$  is the power pulse length;  $\delta$  is the Dirac delta function;  $H$  is the heavyside function.

$$\delta(r) = \begin{cases} 0, & r \neq 0 \\ 1, & r = 0 \end{cases} \quad H(x) = \begin{cases} 0, & x \leq 0 \\ 1, & x > 0 \end{cases}$$

Based on pre-described PSM model, the probe temperature (temperature at  $r = 0$ ) can be solved as

$$\theta(0, t) = \frac{\gamma}{k_t^{1.5}} \int_0^\Phi (t - s)^{-1.5} \cdot e^{-\beta(t-s)} ds$$

where

$$\beta = \frac{W_b C_b}{\rho_t C_t} \quad \gamma = q_p (\rho_t C_t)^{0.5} / 8\pi^{1.5} \quad \phi = \begin{cases} t, & t \leq t_p \\ t_p, & t > t_p \end{cases}$$

For the SSM model introduced by Diederich et al. [19], it is assumed that the probe bead is of spherical, and the power applied to the probe bead is of finite extent and is uniformly distributed in a sphere with a radius equal to the outer bead radius, and the  $q_b$  takes the form as:

$$q_b = q_p [1 - H(r - a)] \cdot [1 - H(t - t_p)] \quad (5)$$

where  $a$  is the radius of the probe bead.

A Green’s function analysis was used to solve the SSM model, for the central temperature of the probe bead (temperature at  $r = 0$ ):

$$\theta(0, t) = \eta \int_0^\phi e^{-\beta(t-s)} \left\{ \operatorname{erf} \left( \frac{a}{\sqrt{4\alpha_t(t-s)}} \right) - \frac{a}{\sqrt{\pi\alpha_t(t-s)}} e^{-\frac{a^2}{4\alpha_t(t-s)}} \right\} ds \quad (6)$$

where  $\alpha_t$  is the thermal diffusivity of tissue.

$$\alpha_t = \frac{k_t}{\rho_t C_t} \quad \eta = \frac{q_p}{\rho_t C_t} \quad \phi = \begin{cases} t, & t \leq t_p \\ t_p, & t > t_p \end{cases}$$

Because the probe thermistor bead sensing temperature is the average temperature of the whole bead [10], SSM model replaces the probe average temperature with the probe central temperature when Eq. (6) is used to estimate the blood perfusion, which would certainly account for one of the main error sources for the blood perfusion prediction. Therefore, a novel ATM (average temperature model) model is presented in this paper, in which the average temperature analytical solution of the probe bead is used to estimate the blood perfusion based on the thermal pulse decay method, and the measurement accuracy are expected to be improved.

Using the same assumption as the SSM model,  $q_b$  still takes the form of Eq. (5). According to the Green's function analysis [21], the temperature field can be solved as:

$$\begin{aligned} \theta(r,t) = & \frac{q_p}{2(k_t/\alpha_t)} \int_0^\phi e^{-\beta(t-s)} \left\{ \operatorname{erf} \left( \frac{r+a}{2\sqrt{\alpha_t(t-s)}} \right) \right. \\ & - \operatorname{erf} \left( \frac{r-a}{2\sqrt{\alpha_t(t-s)}} \right) + \frac{2\sqrt{\alpha_t(t-s)}}{\sqrt{\pi} \cdot r} \\ & \left. \times \left[ \frac{e^{-\frac{(r+a)^2}{4\alpha_t(t-s)}}}{\sqrt{\alpha_t(t-s)}} - \frac{e^{-\frac{(r-a)^2}{4\alpha_t(t-s)}}}{\sqrt{\alpha_t(t-s)}} \right] \right\} ds. \end{aligned} \quad (7)$$

The average temperature of the probe bead,  $\theta_{ave}$  can be yielded by integrating the probe temperature  $\theta(r,t)$  from zero to the radius of the bead.

$$\theta_{ave}(t) = \frac{\int_0^a \theta(r,t) \cdot 4\pi \cdot r^2 dr}{\frac{4}{3}\pi \cdot a^3}. \quad (8)$$

Substitution of Eq. (7) for Eq. (8), the average temperature of the bead can be derived as:

$$\begin{aligned} \theta_{ave}(t) = & q_p \int_0^\phi e^{-\beta(t-s)} f(s) ds \\ f1(s) = & 4 \frac{(\alpha_t(t-s))^{3/2}}{a\sqrt{\pi}} \\ & + \left( -4 \frac{(\alpha_t(t-s))^{3/2}}{a} + 2a\sqrt{\alpha_t(t-s)} \right) \\ & \times \left( \frac{1}{\sqrt{\pi}} \frac{e^{-\frac{a^2}{4\alpha_t(t-s)}}}{\sqrt{\alpha_t(t-s)}} - \frac{a}{\sqrt{\alpha_t(t-s)}} \operatorname{erfc} \left( \frac{a}{\sqrt{\alpha_t(t-s)}} \right) \right) \\ f2(s) = & f1(s) - 4\alpha_t(t-s) \operatorname{erfc} \left( \frac{a}{\sqrt{\alpha_t(t-s)}} \right) - 6a\sqrt{\frac{\alpha_t(t-s)}{\pi}} \\ f(s) = & f2(s) \frac{\alpha_t}{2a^2 k_t} + \frac{\alpha_t}{k_t} \\ \phi = & \begin{cases} t, & t \leq t_p \\ t_p, & t > t_p \end{cases} \end{aligned}$$

In the deriving process, the PSM model did not take into account the size of the probe bead and both the SSM model and the ATM model presented in this paper assumed the thermal properties of the tissue and the probe bead are equal, and besides, the blood perfusion is assumed to exist in the probe bead and equal to the blood perfusion of tissue. These assumptions are the sources for the model error (theoretical error) in the measurement of the blood perfusion for each model. In order to analyze these model errors and compare the accuracy of each model, a numerical experiment method is used.

### 3. Numerical experiment

So-called numerical experiment is to model the probe bead and surrounding tissue separately based on the heat transfer characteristics. The probe bead, which in reality is a composite prolate spheroid, is taken as a sphere and the electrical power is assumed uniformly distributed throughout the bead [10], in which the heat transfer form is through the heat conductivity. The tissue is modeled as a concentric spherical region surrounding the bead in which the heat transfer process can be described by the bio-heat transfer equation. The thermal properties of the probe bead and the tissue can be chosen according to each property, thus various desired bead–tissue systems can be simulated. The blood perfusion rate of the tissue can also be chosen for different values to simulate different physiological states. This kind of handling can be considered to describe the actual physical characters more accurately. The finite difference method is used to solve the two coupling models of the bead and the tissue. The average temperature of the bead calculated from the numerical experiment would be a more accurate representation of the actual thermal response of the probe bead than the analytical temperature solution calculated from the PSM model, the SSM model, and the ATM model, and can be simulated as the actual measurement data to calculate the predicting blood perfusion by using the PSM, SSM, and ATM models, respectively. This kind of analysis method has been used by Diederich et al. [19] to systematically evaluate the accuracy of the PSM and SSM models, but the detailed performance was not given, which is shown as the follows.

The temperature field of the bead can be described by the partial differential heat conduction equation.

$$\frac{k_p}{r^2} \frac{\partial}{\partial r} \left( r^2 \frac{\partial \theta_p}{\partial r} \right) + q_b = \rho_p C_p \left( \frac{\partial \theta_p}{\partial t} \right) \quad r \leq a \quad (9)$$

where  $\rho_p$ ,  $C_p$ ,  $k_p$  denote the density, specific heat, and the thermal conductivity of the probe bead.

The temperature field of tissue can be described by Eq. (3).

$$\frac{k_t}{r^2} \frac{\partial}{\partial r} \left( r^2 \frac{\partial \theta_t}{\partial r} \right) - W_b C_b \theta_t = \rho_t C_t \left( \frac{\partial \theta_t}{\partial t} \right) \quad r > a \quad (10)$$

The initial conditions and boundary conditions are:

$$\theta_p = 0; \theta_t = 0 \quad \text{for } t = 0 \quad (11a)$$

$$\frac{\partial \theta_p}{\partial r} = 0 \quad \text{for } r = 0 \quad (11b)$$

$$-k_p \frac{\partial \theta_p}{\partial r} = -k_t \frac{\partial \theta_t}{\partial r} \quad \theta_p = \theta_t \quad \text{for } r = a \quad (11c)$$

$$\theta_t = 0 \quad \text{for } r \rightarrow \infty. \quad (11d)$$

Eqs. (9), (10) and (11) can be solved by using the finite difference method. After the probe bead temperature field  $\theta_p(r, t)$  have been calculated, the average temperature of the bead can be obtained based on Eq. (8).

In order to validate the correctness of the numerical solutions, the numerical calculation is compared with the analytical solution for some selected cases. As discussed, on condition that the thermal properties of the probe bead and of the tissue are equal, and the blood perfusion in the tissue is assumed to be zero, the numerical solution of the probe bead average temperature obtained from the numerical experiment should be equal to the analysis solution solved from the ATM model. Fig. 1 shows the bead average temperature-varying curves calculated from the ATM model and from the numerical experiment. The parameters used are:  $k_t = k_p = 0.6 \text{ W/m}^\circ\text{C}$ ,  $\alpha_t = \alpha_p = 1.5 \times 10^{-7} \text{ m}^2/\text{s}$ ,  $a = 0.2 \text{ mm}$ ,  $W_b = 0$ ,  $t_p = 3 \text{ s}$ , and an applied power of 4 mW. As illustrated in Fig. 1, the numerical experiment results virtually overlap the analytic solutions from the ATM model.

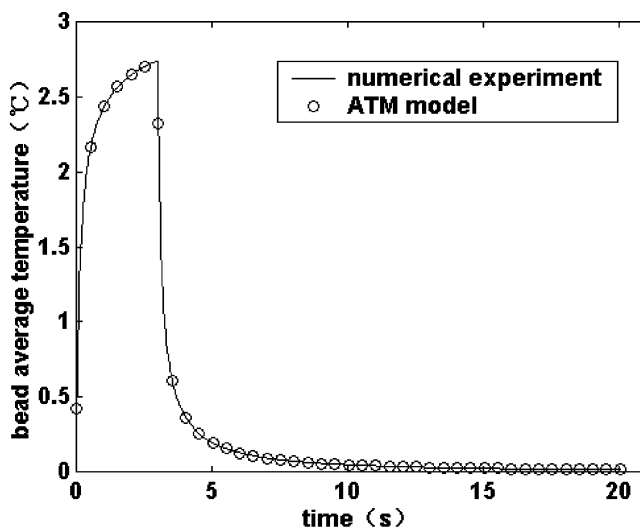


Fig. 1. Temperature varying curve produced from the numerical experiment and ATM model.

Using the probe bead average temperature data generated by the numerical experiment, the least-squares regression is applied to predict the blood perfusion based on the PSM, SSM, and ATM models, respectively, by minimizing the difference between the temperature data calculated from the numerical experiment and the theoretically calculated temperature. The model error (theoretical error) of each model can be calculated by comparing the predicted value with the known blood perfusion value pre-chosen in the numerical experiment.

To investigate the dependence of the model error on time  $t_m$  at which the blood perfusion is measured, the temperature data, which are measured from an interval of 1.0 s, centered at the desired measurement time  $t_m$ , are used. For example, in the numerical experiment, the blood perfusion estimated at 9 s after the pulse is calculated by using the temperature data from 8.5 to 9.5 s after the pulse.

In the numerical experiment, the parameters are chosen as follows, unless noted otherwise. The tissue parameters:  $k_t = 0.5 \text{ W/m}^\circ\text{C}$ ,  $\alpha_t = 1.4 \times 10^{-7} \text{ m}^2/\text{s}$ ,  $W_b = 5\text{--}30 \text{ kg/m}^3 \text{ s}$ . According to Diederich et al. [19], the bead parameters are:  $k_p = 7 \text{ W/m}^\circ\text{C}$ ,  $C_p = 835 \text{ J/kg}^\circ\text{C}$ ,  $\rho_p = 2225 \text{ kg/m}^3$ . The radius of the probe bead  $a = 0.2 \text{ mm}$ , the pulse length  $t_p = 3 \text{ s}$ , the measurement time is 9 s after the pulse, and an applied power of 4 mW.

#### 4. Results

The effects of measurement time, blood perfusion rate, tissue thermal conductivity, tissue thermal diffusivity, probe bead radius, probe bead thermal conductivity, and pulse length on the prediction errors of the blood perfusion were shown in Figs. 2–7 for each ana-

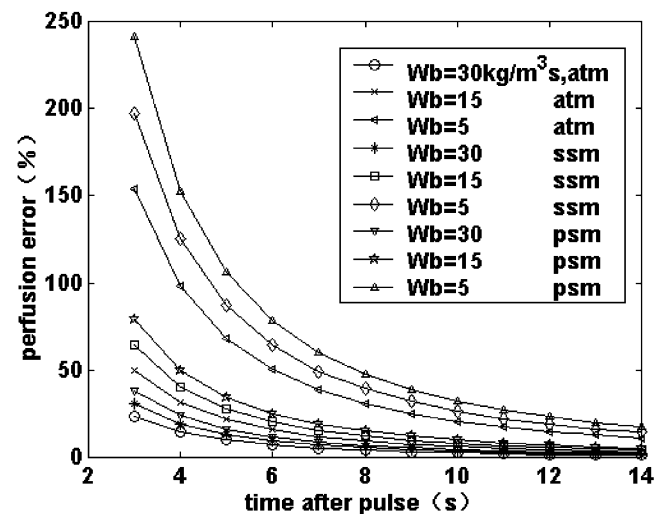


Fig. 2. Blood perfusion prediction error at different measurement times.

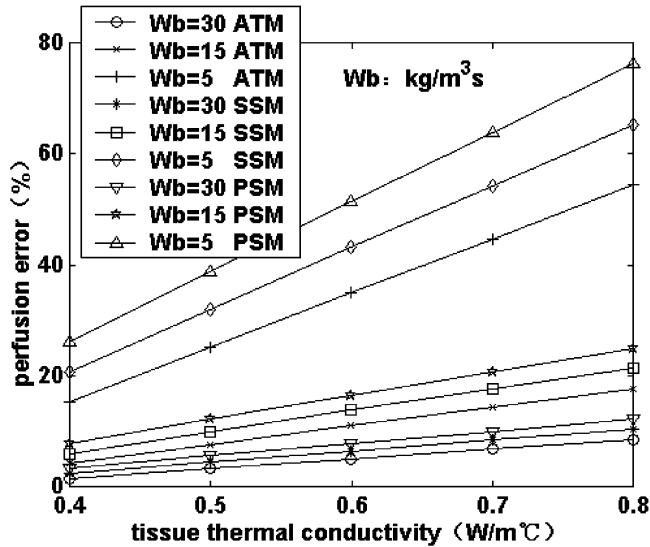


Fig. 3. Effects of tissue thermal conductivity on blood perfusion prediction errors.

lytical model. The blood perfusion rate used in the numerical experiment, for each case is 5, 15, and 30  $\text{kg}/\text{m}^3\cdot\text{s}$ , respectively.

The situations that the predicting blood perfusion errors vary with measurement time are shown in Fig. 2 for various blood perfusion rates. For a short time after the pulse, the blood perfusion error for each model is large. As the measurement time increases, the blood perfusion prediction error decreases. When measurement time is long, an acceptable result can be achieved. That is, for measurement times larger than 9 s after the pulse, the blood perfusion error for ATM model would be smaller than 15% for blood perfusion of 15  $\text{kg}/\text{m}^3\cdot\text{s}$  or greater. As the blood perfusion rate

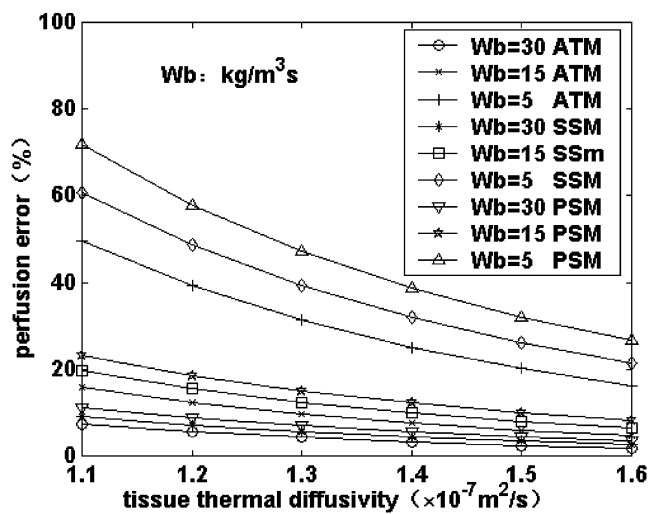


Fig. 4. Effects of tissue thermal diffusivity on blood perfusion prediction errors.

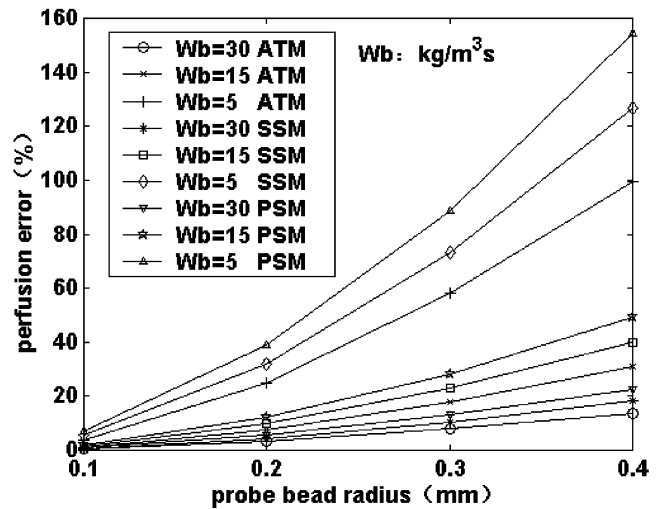


Fig. 5. Effects of probe bead radius on blood perfusion prediction errors.

increases, the blood perfusion prediction error also decreases. The blood perfusion prediction error for low blood perfusion rate is much larger than that for the moderate and high blood perfusion rate, and longer measurement time should be chosen in order to reach the same accuracy as the moderate and high blood perfusion rate. Among the three analytical models, for various blood perfusion rates, the prediction error for the PSM model belongs to the largest, and the prediction error for the ATM model is the smallest.

To show the effects of the tissue thermal properties, the perfusion error is plotted against tissue thermal conductivity and tissue thermal diffusivity in Figs. 3 and 4, respectively. The measurement time is 9 s after the pulse. The tissue thermal conductivity varies from

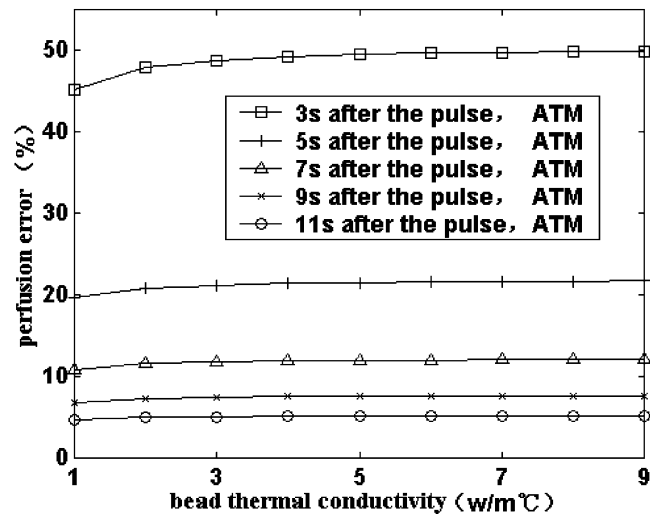


Fig. 6. Effects of probe bead thermal conductivity on blood perfusion prediction errors.

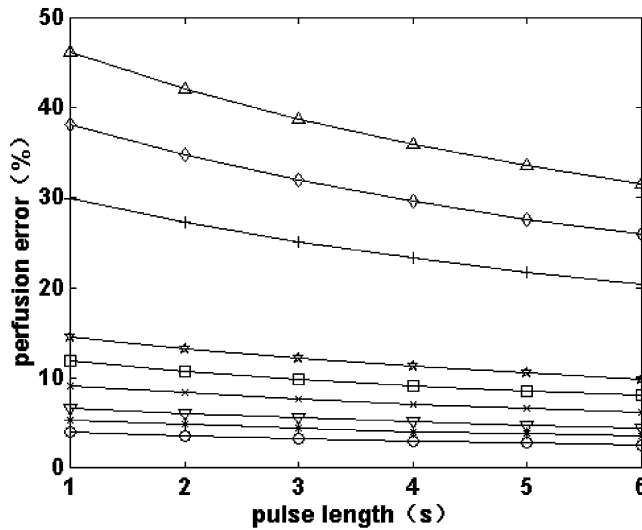


Fig. 7. Effects of pulse length on blood perfusion prediction error. The legend is the same as Fig. 5.

0.4 to 0.8  $\text{W/m}^\circ\text{C}$ , the tissue thermal diffusivity varies from  $1.1 \times 10^{-7} \text{ m}^2/\text{s}$  to  $1.6 \times 10^{-7} \text{ m}^2/\text{s}$ , which covers a wide range of the tissue thermal properties. As shown in the figures, the smaller tissue thermal conductivity and the larger tissue thermal diffusivity would diminish the blood perfusion prediction error. Again, the blood perfusion prediction error is larger at low blood perfusion rate, and among the three analytical models, the prediction error for the ATM model is the smallest.

The effects of the probe bead parameters are given in Figs. 5 and 6. It is evident that the bead radius has a significant effect on the prediction of the blood perfusion, and the smaller values of the bead radius would reduce the blood perfusion prediction error obviously. The larger blood perfusion rate and ATM model are again found to produce smaller blood perfusion errors. Fig. 6 shows the effects of the bead thermal conductivity on the blood perfusion predicted using ATM model. The blood perfusion used in the numerical experiment is  $15 \text{ kg/m}^3\cdot\text{s}$ , the measurement time is from 3 to 11 s after the pulse, the bead thermal conductivity varies from 1 to 9  $\text{W/m}^\circ\text{C}$ . For a short time after the pulse, the blood perfusion error is slight smaller at low values of the bead thermal conductivity, and the blood perfusion errors for moderate and large values of the bead thermal conductivity are almost at the same value. Furthermore, when the measurement time is long, the differences of the blood perfusion errors for various bead thermal conductivities could be ignored. For other blood perfusion rates used in the numerical experiment, the same tendencies could be found.

To show the effects of the pulse length, the blood perfusion error of each model versus the pulse lengths used in the numerical experiment is shown in Fig. 7.

The pulse length varies from 1 to 6 s. It is evident that the longer pulse length will produce better results for low blood perfusion rates. For the moderate and high blood perfusion rate, the blood perfusion prediction error also decrease with the increase in the pulse length, however, the effects are not obvious. Again, the blood perfusion prediction error is larger at low blood perfusion rate, and among the three analytical models, the prediction error for the ATM model is the smallest.

## 5. Discussion

When the pulse-decay method is used to measure the blood perfusion of tissue, as the measurement time is increasing, the effective measurement volume of tissue also enlarges. The temperature response of the probe bead represents the integrative influences of the probe bead parameters and the thermal properties of the effective measurement volume of tissue. As shown in Fig. 2, when the measurement time is short, the blood perfusion prediction errors for each of the three analytical models are large. For the PSM model, it is mainly the results of the finite radius of the probe bead. For this short measurement time, the effective measurement volume of tissue is small, compared to the effective measurement volume of tissue, the effect of the dimension of the probe bead cannot be ignored, and the bead cannot be regard as a point heat source. For the SSM and ATM models, it is mainly the results that the thermal properties of the tissue and the probe bead are not equal and the blood perfusion does not exist in the probe bead. However, as the measurement time increases, the effective measurement volume of tissue enlarges, the rate of the probe bead dimension to the effective measurement volume of tissue decreases, and the effects of the finite radius of the probe bead are weakened. At the same time, the effects of the differences in the thermal properties between the probe bead and the tissue are also weakened. Therefore, the prediction error for each of the three analytical models decreases with the increase in measurement time. Among the three analytical models, the ATM model takes the effects of the probe bead dimensions into account and describes the actual physical characteristics best; that is, the average temperature solution of the bead is derived and used to estimate the blood perfusion by the ATM model. Therefore, the prediction error for the ATM model is the smallest for all the conditions tested.

Similarly, for the same measurement time, the effective measurement volume of tissue enlarges with the increase in the tissue thermal diffusivity, for reasons mentioned previously, the larger value of the tissue thermal diffusivity will also result in a better blood perfusion prediction, shown as Fig. 4. When the longer

pulse length is chosen and the measurement time is maintained at the same value after the pulse, the overall measurement interval will increase. For example, the pulse length is chosen as 3 and 5 s, respectively, and the measurement time is 9 s after the pulse, then, the overall measurement interval is 12 and 14 s, respectively. Due to the increase of the overall measurement interval, the effective measurement volume of tissue would also enlarge. Consequently, the longer pulse length will produce better prediction results, shown as Fig. 7.

For the same measurement time, the effective measurement volume of tissue would be almost unchanged provided that the thermal properties of the tissue are maintained at fixed values. Consequently, the rate of the probe bead dimension to the effective measurement volume of tissue would decrease when smaller probe bead radius is chosen. As a result, the effects of the finite radius of the probe bead and the effects of the differences in the thermal properties between the probe bead and the tissue would be weakened. The improved effect of decreasing the probe bead radius on the blood perfusion measurement is most noticeable, which can be disclosed by the following simple calculation. If the bead radius is decreased from 0.3 to 0.2 mm and all the other parameters are maintained at fixed values, the rate of the probe bead dimension to the effective measurement volume of tissue would decrease approximately 33%. Therefore, it could improve the measurement accuracy significantly if small probe bead radius is chosen, shown as Fig. 5.

Eq. (10) can be transformed to the following form

$$\frac{1}{r^2} \frac{\partial}{\partial r} \left( r^2 \frac{\partial \theta_t}{\partial r} \right) - \frac{W_b C_b}{k_t} \theta_t = \frac{1}{\alpha_t} \left( \frac{\partial \theta_t}{\partial t} \right) \quad r > a. \quad (12)$$

In Eq. (12),  $(W_b C_b / k_t) \theta_t$  represents the contributions of the blood perfusion for the heat transfer of tissue, and is called the blood perfusion term. On condition that the other parameters are unchanged, the coefficient of the blood perfusion term,  $W_b C_b / k_t$ , would increase with the increase in the blood perfusion rate, the result is that the larger blood perfusion rate would have more influence on the thermal response of the probe bead, and the measured temperature curve reveals more information on the blood perfusion of the tissue. Therefore, the blood perfusion prediction accuracy would be enhanced with the increase in the blood perfusion measured. For the low rate of blood perfusion, the blood perfusion term in Eq. (12) is much smaller in scalar, and the heat transfer of tissue is dominated by the thermal conduction mode [14], the contributions of the blood perfusion for the probe bead thermal response is so low too, thus the prediction error is large.

Again, if the thermal conductivity of the tissue decreases, the coefficient of the blood perfusion term,

$W_b C_b / k_t$ , would also increase which, for the same reason as mentioned above, would make the blood perfusion prediction become more accurate, shown as Fig. 3.

These conclusions can also be demonstrated by studying the analytical solutions of the three models more carefully. The factor of  $e^{-\beta(t-s)}$  is involved in every solution, which represents the contributions of the blood perfusion for the thermal response of probe bead directly, where

$$\beta = \frac{W_b C_b}{\rho_t c_t} = \frac{W_b C_b \alpha_t}{k_t}.$$

It is evident that an increase in blood perfusion and tissue thermal diffusivity, a decrease in tissue thermal conductivity, would all enlarge the value of  $\beta$ , thus strengthen the effects of the blood perfusion on the probe bead thermal response, and make the sensed temperature decay curve represent more information of the blood perfusion measured. Therefore, the larger blood perfusion, the larger tissue thermal diffusivity, and the smaller tissue thermal conductivity, could all produce better prediction of the blood perfusion.

It seems there are some inconsistencies compared to the report of Diederich et al. [19], in which it was found that the larger values of tissue conductivity decrease the error for predicting perfusion. It is noticed that the effects of the tissue thermal conductivity was studied on condition that the density and the specific heat of tissue were maintained unchanged in their paper. However, in this paper, the effects of the tissue thermal conductivity is studied on condition that the tissue thermal diffusivity is maintained unchanged. For the condition applied by Diederich et al., in fact, they studied the effects of the tissue thermal diffusivity on the error for predicting blood perfusion, which is accorded with the conclusions in this paper.

For long measurement time, the effective measurement volume of tissue is large which, for reasons mentioned previously, allow some probe bead parameters to be ignored [19]. As shown in Fig. 5, the predicting errors for different bead thermal conductivity are nearly equal as the long measurement times is reached, which means the predicting error is independent of the bead thermal conductivity for these long measurement times.

As has been revealed, the longer measurement time would reduce the model error of blood perfusion prediction, hence reduce the overall measurement error of blood perfusion, and produce better results. However, for the thermal pulse-decay method, the probe bead sensed signal is decreasing gradually in the measurement period (power-off and temperature decay period), thus the blood perfusion measurement error caused by the error in the measured temperature would gradually increase [18], which would increase the overall

measurement error. Therefore, there is an optimum value for the measurement time. By considering the two aspects of the effects of the measurement time on the overall measurement errors, the 9 s after the pulse is chosen to be the typical measurement time in this paper. It is also the reason why a probe bead radius smaller than 0.2 mm is not chosen in practice, because the temperature of the bead will decay faster.

For the typical measurement time, the corresponding radius of the effective measurement tissue is small (about 5 to 10 mm). Therefore, the thermal conductivity and the thermal diffusivity can be assumed to be uniform within the tissue measured, as has been determined by Arkin et al. [13]; and the measurement result represents the local perfusion despite the distribution of blood perfusion within an organ may not be uniform, which is one of the advantages of the thermal pulse decay method.

For the measurement of low blood perfusion, say,  $W_b < 1 \text{ kg/m}^3 \cdot \text{s}$ , as has been mentioned previously, the heat transfer in the tissue is dominated by the thermal conduction mode, and the signal intensity of the blood perfusion is weak. Therefore, the measurement of low blood perfusion is difficult. The numerical experiment also discloses that, for low blood perfusion, the predicting error for ATM model is 20–30% smaller than that for SSM model, and 40–60% smaller than that for PSM model for the typical measurement time (9 s after the pulse). Clearly, it is more beneficial to use the ATM model to measure the low blood perfusion. It is noticed that the probe bead temperature decays slower for low blood perfusion than for moderate and high blood perfusion, therefore, it could improve the prediction accuracy by choosing longer measurement time properly. Furthermore, when the low blood perfusion is measured, using smaller probe bead radius, and choosing longer pulse length, would also produce better results.

## 6. Conclusion

A new average temperature model (ATM) is presented in this paper to measure the blood perfusion of tissue based on the pulse-decay method. For this ATM model, the probe bead average temperature solution is derived and used to estimate blood perfusion. A numerical experiment method is used to study the prediction model errors for the point source model, the spherical source model, and the average temperature model. For all the cases tested, the ATM model is more accurate than the other two. When the ATM model is used to measure the tissue blood perfusion, the prediction errors decrease with the increase in the measurement time, tissue blood perfusion, tissue thermal diffusivity, the pulse length, and increase with the increase in tissue thermal conductivity and probe bead

radius. Considering the model error and the measurement error caused by the error in measured temperature, the measurement time is preferred as 9 s after the pulse. For this typical measurement time, the effects of the bead thermal conductivity on the prediction error could be ignored. To improve measurement accuracy, the smaller probe bead radius and longer pulse length should be chosen properly. For the measurement of low blood perfusion, the predicting error for ATM model is 20–30% smaller than for SSM model, and 40–60% smaller than PSM model for the typical measurement time, additionally, a longer measurement time can be chosen to produce better results.

## Acknowledgements

The present work is financially supported by the key project of the National Natural Science Foundation of China under grant No. 59836240.

## References

- [1] Arkin H, Xu LX, Holmes KR. Recent developments in modeling heat transfer in blood perfused tissues. *IEEE Trans Biomed Eng* 1994;41:97–107.
- [2] Martin GT, Haddad MG, Cravalho EG, Bowman HF. Thermal model for the local microwave Hyperthermia treatment of benign prostatic hyperplasia. *IEEE Trans Biomed Eng* 1992;39:836–44.
- [3] Charny CK, Levin RL. A three-dimensional thermal and electromagnetic model of whole limb heating with a MAPA. *IEEE Trans Biomed Eng* 1991;38:1030–9.
- [4] Kim B-M, Jacques SL, Rastegar S, Thomsen S, Motamedi M. Nonlinear finite-element analysis of the role of dynamic changes in blood perfusion and optical properties in laser coagulation of tissue. *IEEE J Select Top Quant Electron* 1996;2:922–33.
- [5] Habler OP, Messmer KF. Tissue perfusion and oxygenation with blood substitutes. *Adv Drug Del Rev* 2000;40:171–84.
- [6] Ng EYK, Chua LT. Comparison of one- and two-dimensional programmes for predicting the state of skin burns. *Burns* 2002;28:27–34.
- [7] Tharp HS, Roemer RB. Optimal power deposition with finite-sized, planar hyperthermia applicator arrays. *IEEE Trans Biomed Eng* 1992;39:569–79.
- [8] Tompkins DT, Vanderby R, Klein SA, Beckman WA, Steeves RA, Paliwal BR. Effects of interseed spacing, tissue perfusion, thermoseed temperatures and catheters in ferromagnetic hyperthermia: results from simulations using finite element models of thermoseeds and catheters. *IEEE Trans Biomed Eng* 1994;41:975–85.
- [9] Diederich CJ, Burdette EC. Transurethral ultrasound array for prostate thermal therapy: initial studies. *IEEE Trans Ultrason Ferroelect Freq Control* 1996;43:1011–22.
- [10] Valvano JW, Allen JT, Bowman HF. The simultaneous measurement of thermal conductivity, thermal diffusivity, and perfusion in small volumes of tissue. *J Biomech Eng* 1984;106:192–7.
- [11] Valvano JW, Allen JT, Walsh JT, Hnatowich DJ, Tomera JF, Brunengraber H, Bowman HF. An isolated rat liver model for

- the evaluation of thermal techniques to quantify perfusion. *J Biomech Eng* 1948;106:187–91.
- [12] Newman WH, Lele PP. A transient heating technique for the measurement of thermal properties of perfused biological tissue. *J Biomech Eng* 1985;107:219–27.
- [13] Arkin H, Holmes KR, Chen MM, Bottje WG. Thermal pulse decay method for simultaneous measurement of local thermal conductivity and blood perfusion: a theoretical analysis. *J Biomech Eng* 1986;108:208–14.
- [14] Kress R, Roemer R. A comparative analysis of thermal blood perfusion measurement techniques. *J Biomech Eng* 1987;109: 218–25.
- [15] Patel PA, Valvano JW, Pearce JA, Prahl SA, Denham CR. A self-heated thermistor technique to measure effective thermal properties from the tissue surface. *J Biomech Eng* 1987;109: 330–5.
- [16] Sarit AS, Vil B, Thalia K, Solange A. A combined heat clearance method for tissue blood flow measurement. *J Biomech Eng* 1991;113:438–45.
- [17] Anderson GT, Valvano JW, Santos RR. Self-heated thermistor measurement of perfusion. *IEEE Trans Biomed Eng* 1992;39: 877–85.
- [18] Arkin H, Holmes KR, Chen MM. A sensitivity analysis of the thermal pulse decay method for measurement of local tissue conductivity and blood perfusion. *J Biomech Eng* 1986;108:54–8.
- [19] Diederich CJ, Clegg S, Roemer RB. A spherical source model for the thermal pulse decay method of measuring blood perfusion: a sensitivity analysis. *J Biomech Eng* 1989;111:55–61.
- [20] Pennes HH. Analysis of tissue and arterial blood temperatures in the resting human forearm. *J Appl Physiol* 1948;1:93–122.
- [21] Ozisik MN. Heat conduction. New York: Wiley; 1981.